

# Čerenkov Photon Density Fluctuations in Extensive Air Showers

V. R. Chitnis and P. N. Bhat  
*Tata Institute of Fundamental Research,  
Homi Bhabha Road, Mumbai 400 005, India.*

October 1, 2018

## Abstract

The details of Čerenkov light produced by a  $\gamma$ -ray or a cosmic ray incident at the top of the atmosphere is best studied through systematic simulations of the extensive air showers. Recently such studies have become all the more important in view of the various techniques resulting from such studies, to distinguish  $\gamma$ -ray initiated showers from those generated by much more abundant hadronic component of cosmic rays. We have carried out here such systematic simulation studies using CORSIKA package in order to understand the Čerenkov photon density fluctuations for 5 different energies at various core distances both for  $\gamma$ -ray and proton primaries incident vertically at the top of the atmosphere. Such a systematic comparison of shower to shower density fluctuations for  $\gamma$ -ray and proton primaries is carried out for the first time here. It is found that the density fluctuations are significantly non-Poissonian. Such fluctuations are much more pronounced in the proton primaries than  $\gamma$ -ray primaries at all energies. The processes that contribute significantly to the observed fluctuations have been identified. It has been found that significant contribution to fluctuations comes from photons emitted after shower maximum. The electron number fluctuations and correlated emission of Čerenkov photons are mainly responsible for the observed fluctuations.

## 1 Introduction

Ground based atmospheric Čerenkov technique is, at present, the only way by which TeV  $\gamma$ -rays could be detected from point sources such as  $\gamma$ -ray pulsars, short period X-ray binaries or BL-Lac objects. Recent detection of TeV emission from a few of these objects (Vacanti *et al.*, 1991; Punch *et al.*, 1992,

Chadwick *et al.*, 1997, Quinn *et al.*, 1997, Weekes, 1988, Fegan, 1994) has created much interest in the field of TeV  $\gamma$ -ray astronomy. The  $\gamma$ -ray signals found typically are  $\sim 1\%$  of the more abundant background events of cosmic ray nuclei, particularly protons. In order to detect faint Very High Energy (VHE)  $\gamma$ -ray sources, one has to improve the signal to noise ratio by rejecting the bulk of the hadronic background. In order to do so it is imperative to study the detailed characteristics of Čerenkov light production by photon initiated and proton initiated cascades in the atmosphere.

Simulation studies in the past (Rao & Sinha, 1988; Hillas & Patterson, 1987; Zatsepin & Chudakov, 1962) have shown that the Čerenkov pool at the observation level has the signature of the primary. The lateral distribution of Čerenkov radiation seems to be distinctly different in  $\gamma$ -ray and proton initiated showers in the sense that in the former case it is flat upto about 140 m and characterized by an increased photon density (called the ‘hump’) at that distance while in the latter case it is steeper with practically no hump. It has been suggested (Rao & Sinha, 1988) that this characteristic difference could be measured in an observation and could be used for improving the signal to noise ratio. These arguments are based on the average properties of showers. In practice, however, Čerenkov photon density fluctuations play a dominant role. The signature of the primary gets buried in the noise which is mainly due to large fluctuations in photon densities from shower to shower, even at same energy. These fluctuations in turn reduce the efficiency by which the primary could be identified based on the lateral distribution measurements (Krys and Wasilewski, 1993). As a result, the study of the photon fluctuations plays an important role in deciding the signal to noise ratio of the VHE  $\gamma$ -ray observations based on the measurement of lateral distribution of Čerenkov light.

It has been known that shower to shower fluctuations in proton initiated cascades are expected to be much larger than  $\gamma$ -ray initiated cascades since the nuclear interaction mean free path ( $70 \text{ g cm}^{-2}$ ) is about twice as large as the radiation length ( $37.15 \text{ g cm}^{-2}$ ) in the atmosphere and the number of secondaries and their energy spectra are known to fluctuate widely. Furthermore muons, which are present only in hadron initiated showers (above the Čerenkov threshold  $E_\mu \sim 4 \text{ GeV}$ ) reach the observation level and could create local peaks in the light pool at the observation level (Hillas & Patterson, 1987). In this paper we make an attempt to estimate and compare the extent of these fluctuations in proton and  $\gamma$ -ray initiated showers at various energies and estimate the relative contributions from different but known sources of fluctuations.

## 2 The Simulations

We have used CORSIKA package version 4.502 (Knapp & Heck, 1995) for simulation of air showers generated by  $\gamma$ -rays and protons. This package simulates

interactions of nuclei, hadrons, muons, electrons and photons as well as decays of unstable secondaries in the atmosphere. It also provides information about the type, energy, location, direction and arrival times of all the secondary particles generated in the air shower, which reach the observation level. It also supports the option of generating Čerenkov photons emitted by various particles in the shower. It uses the EGS4 package (Nelson *et al.*, 1985) for the development of the electromagnetic cascade in the atmosphere. The Čerenkov radiation produced by the secondary charged particles within the specified bandwidth (300-550 nm) is propagated to the ground. The position, angle, time and production height of each Čerenkov photon hitting the detector at the observation level are recorded. However, the wavelength dependent absorption of these photons in the atmosphere is not taken into account.

In the present work we have studied the Čerenkov light produced by monoenergetic  $\gamma$ - rays and protons incident vertically at the top of the atmosphere. Height of the first interaction is selected randomly taking into consideration the appropriate mean free path. Target of the first interaction is chosen randomly according to atmospheric abundances. In the simulations, we have considered an array of detectors with area  $2.11 \times 2.11 \text{ m}^2$  (this corresponds to the total mirror area of each telescope in the Pachmarhi Array of Čerenkov Telescopes (PACT), see Bhat *et al.* 1997), with 17 detectors in X-direction and 21 detectors in Y-direction. Spacing between the detectors in X-direction is 25 m and in Y-direction is 20 m. It may be mentioned that even though PACT consists of only 25 telescopes each of area  $4.45 \text{ m}^2$ , a larger array is chosen for simulation purposes in order to study core distance dependent properties of PACT. Only those Čerenkov photons which hit any of the detectors of the array at all incident angles are recorded. Observation altitude and magnetic field appropriate for Pachmarhi (longitude:  $78^\circ 26'E$ ; latitude:  $22^\circ 28'N$  and altitude: 1075 m amsl) location are taken into account. The shower core is always chosen to be at the centre of the array.

An option of variable bunch size is available in the package, which defines the number of Čerenkov photons treated together. This will also reduce the size of the output data file. However, it was noticed that for fluctuation studies the bunch size has to be set to unity to get the correct estimate of the fluctuations as larger bunch size tends to overestimate the photon fluctuations.

### 3 Average Čerenkov lateral distributions

Čerenkov photon lateral distributions were generated and averaged over several showers. For various energies of  $\gamma$ - ray and proton primaries, typically 100 showers were generated. For a few energies larger number of showers were generated (e.g. 200 showers for 100 GeV  $\gamma$ - rays and 400 showers for 50 GeV  $\gamma$ - rays and 150 GeV protons) to ensure that average shape of the lateral distri-

bution does not critically depend on the sample size. For 1 TeV  $\gamma$ - rays and 2 TeV protons 50 showers were generated. Fig. 1a shows the average lateral distributions of Čerenkov photons generated by  $\gamma$ - rays of energies 50, 100, 250, 500 and 1000 GeV. Corresponding distribution for protons of energies 150 GeV, 250 GeV, 500 GeV, 1000 GeV and 2000 GeV are shown in fig. 1b. Čerenkov photon densities shown in the plots are averaged over 10 consecutive detectors when arranged with increasing core distance. Proton energies are chosen such that their Čerenkov yield is comparable to that of  $\gamma$ - rays. Even though the average Čerenkov lateral distribution shown in the fig. 1 is derived for the above mentioned detector array, it is verified to be independent of detector size and spacing.

It may be seen that lateral distributions produced by  $\gamma$ - ray primaries show a characteristic hump at a distance of about 135 m from the core for energies of atleast up to 1 TeV. The origin of a hump in the case of  $\gamma$ - ray primaries is discussed in detail by Rao & Sinha (1988). This is due to the focussing of Čerenkov photons from a large range of heights, over which the product of height and Čerenkov angle ( $h\theta_c$ ) is approximately constant. It has also been demonstrated by Rao & Sinha that only the higher energy ( $\geq 1$  GeV) electrons are responsible for the production of the hump. The cumulative RMS scattering angle of these electrons, (which is inversely proportional to the electron energy), is smaller than the Čerenkov angle. Whereas in the case of lower energy electrons this angle is larger than the Čerenkov angle. This enables Čerenkov photons to reach the regions on either side of the hump. In case of proton primaries, electrons are pair produced by  $\gamma$ - rays, which are decay products of  $\pi^0$ s, and have their production angles determined by the transverse momentum of  $\pi^0$ s. This production angle is also to be taken into consideration while calculating the threshold energy of electrons, at which Čerenkov angle is equal to the scattering angle. Hence, this threshold energy for proton primaries is larger than the corresponding value for  $\gamma$ - ray primaries, consequently reducing the relative number of electrons above this threshold. As a result these electrons do not produce a noticeable hump.

Prominence of the hump reduces as the energy of  $\gamma$ - ray primary increases from 50 GeV to 1 TeV, since higher energy electrons penetrate deeper in the atmosphere, thereby increasing the contribution to Čerenkov radiation from electrons from lower altitudes where  $h\theta_c$  starts decreasing (Rao & Sinha, 1988). In order to study the variation of the strength of the hump as a function of primary energy we define the strength of the hump as the ratio of the density at the hump to that at the shower core. We generated nearly 300  $\gamma$ - ray showers of varying energies in the range 50-1000 GeV and computed this ratio for each shower. Fig 2 shows the variation of this ratio with primary  $\gamma$ - ray energy. The ratio decreases with increasing energy as expected and a power law with a slope of -0.38 fits the data well showing that eventually this ratio reduces to a limiting value of 1.

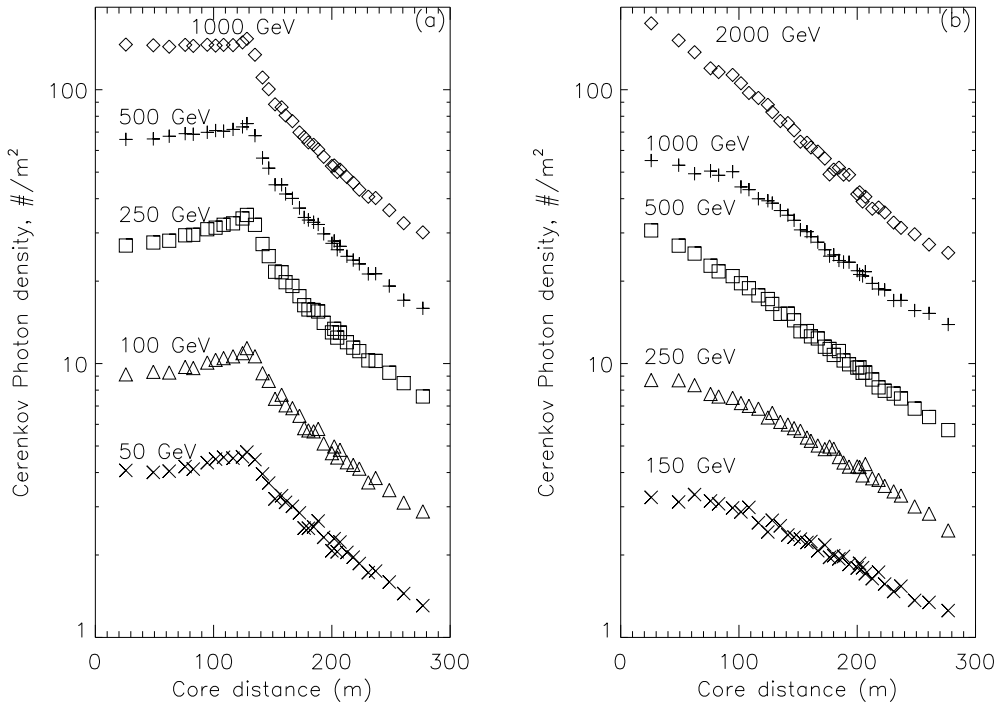


Figure 1: Average lateral distributions of Čerenkov photon densities resulting from extensive air showers initiated by vertically incident (a) $\gamma$ - rays and (b)protons of various energies. Average of 400 showers is used for 50 GeV  $\gamma$ - rays and 150 GeV protons, 200 showers for 100 GeV  $\gamma$ - rays, 100 showers for the rest except for 1 TeV  $\gamma$ - rays and 2 TeV protons for which 50 showers each were simulated.

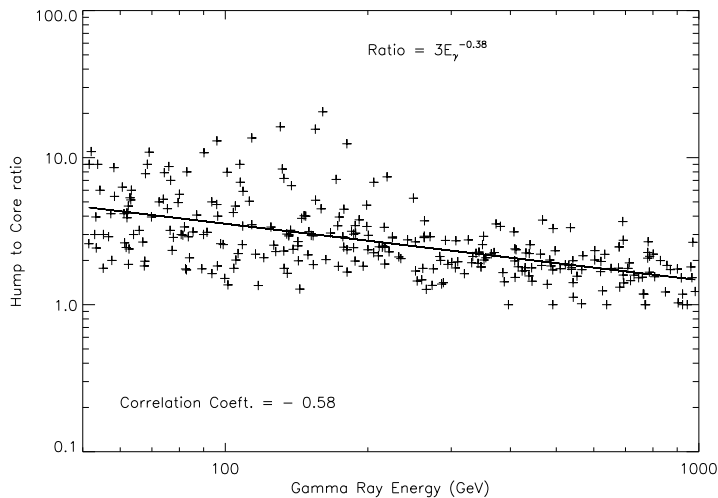


Figure 2: Variation of the ratio of the photon density at the hump to that at the core with primary  $\gamma$ - ray energy. There seems to be a good anticorrelation with energy while the ratio when fitted with a power law has a slope -0.38

Table 1: Least squares fit coefficients for a linear fit to the log of total number of Čerenkov photons as a function of the log of the primary energy for vertically incident  $\gamma$ - rays and protons.

Primary Species	Intercept	Slope
$\gamma$ - rays	$10.53 \pm 0.02$	$1.028 \pm 0.003$
Protons	$9.41 \pm 0.11$	$1.07 \pm 0.02$

## 4 Shower size fluctuations

Figure 3 shows the total number of Čerenkov photons produced in the atmosphere by showers initiated by vertically incident  $\gamma$ - rays and protons of various energies in the range 50 - 1000 GeV, with an assumed energy spectrum of the form,  $E^{-1}$ . Nearly 300 showers each were generated for  $\gamma$ - ray and proton primaries. While there is a very good proportionality between the shower size (hereafter measured in terms of the total number of Čerenkov photons produced in a shower) and primary energy in the case of  $\gamma$ - ray primaries (linear correlation coefficient = 0.998), it is not as good in the case of proton primaries (linear correlation coefficient = 0.9), due to increased fluctuations in the latter case. The best power-law fit parameters to the total number of Čerenkov photons as a function of the primary energy are shown in table 1.

Distributions of the total number of Čerenkov photons produced by  $\gamma$ - ray primaries of energy 100 GeV and 1 TeV and proton primaries of energies 250 GeV

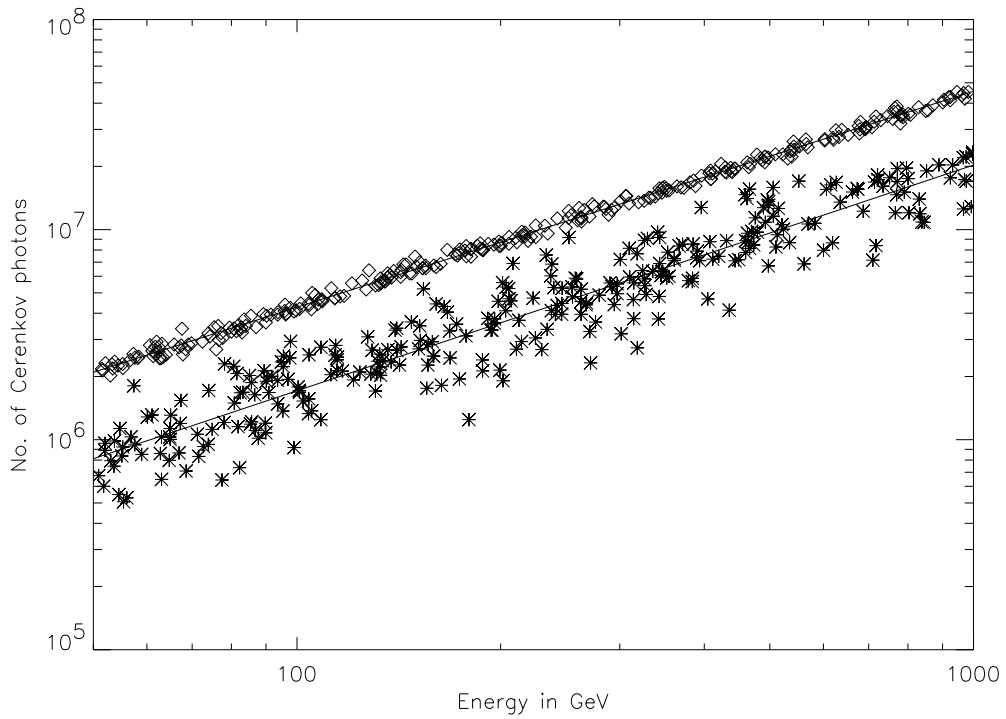


Figure 3: Variation of the total number of Čerenkov photons in the bandwidth 300-550 nm produced by vertically incident  $\gamma$ - rays (diamonds) and protons (stars) with primary energies, indicating the magnitude of photon number fluctuations. The proton generated showers exhibit a significantly higher degree of fluctuations as compared to those by  $\gamma$ - rays.

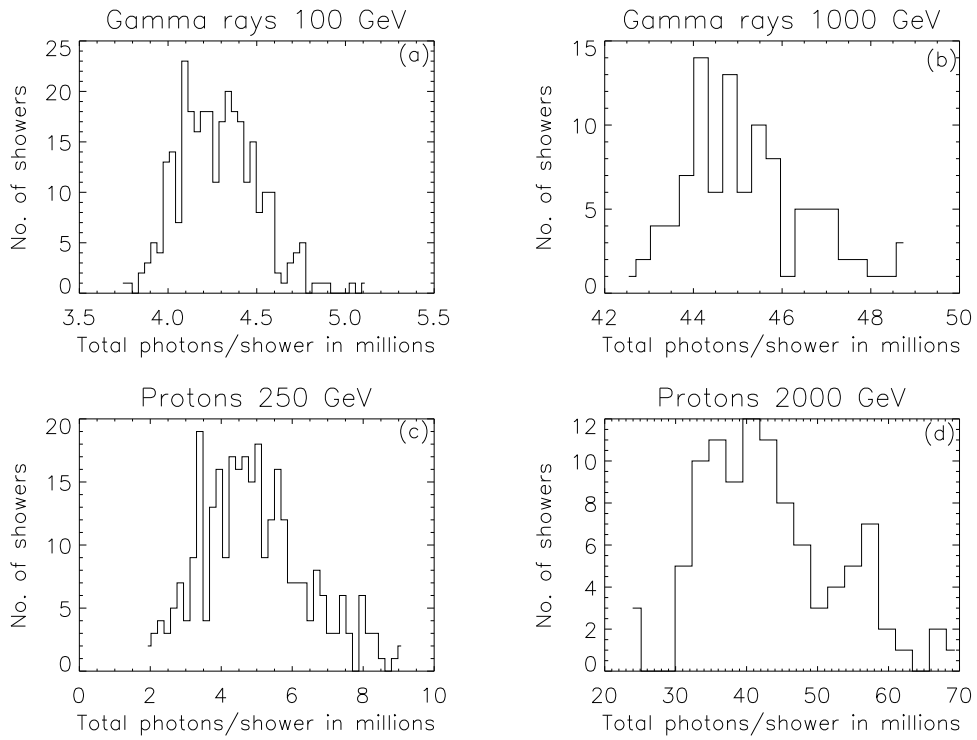


Figure 4: The distributions of the total number of Čerenkov photons in the bandwidth 300-550 nm in showers generated by vertically incident  $\gamma$ - rays and protons each with two different primary energies.



and 2 TeV are shown in fig. 4 a-d respectively. Because of the higher Čerenkov yield from  $\gamma$ -ray primaries (Browning and Turver, 1977), higher energy protons with comparable Čerenkov yields have been chosen for comparison. We have generated 300 showers for lower energy and 100 showers for higher energy  $\gamma$ -rays and protons. Čerenkov photon distributions are much broader for proton primaries compared to those from  $\gamma$ -rays, consistent with fig. 3. The ratio of rms deviation to average number of Čerenkov photons decreases with increasing energy for both  $\gamma$ -rays and protons. When the  $\gamma$ -ray energy increases from 100 GeV to 1000 GeV this ratio falls from 5% to 3%. Similarly when the proton energy increases from 250 to 2000 GeV this ratio falls from 30% to 23%. These results are consistent with those obtained by Ong et al. (1995) (see section 8.2 for details).

## 5 Density fluctuations

### 5.1 Intra-shower fluctuations

Figure 5 shows the variation of the ratio of the absolute deviation to the mean photon density as a function of core distance, averaged over a number of showers. For each shower, average Čerenkov photon densities are calculated over groups of 10 consecutive detectors, when arranged with increasing core distance. Absolute value of the difference between individual photon densities and corresponding mean density is defined as the deviation. Ratio of deviation to the mean density is calculated for each detector, for each shower. Ratios are then averaged over total number of showers (fig. 5). In the case of both  $\gamma$ -rays and protons, ratio of the deviation to the mean photon density increases with core distance. For a given primary, it decreases with increase in the energy of the primary. It is higher by a factor of about 2 for protons of energies in the range 150 GeV - 2 TeV, compared to those for  $\gamma$ -rays of comparable Čerenkov yields. At higher  $\gamma$ -ray energies, i.e., 500 GeV and 1 TeV, there is a sharp increase in the ratio in the hump region. Similar behaviour is also seen in the case of 2 TeV protons.

This ratio can be measured in an atmospheric Čerenkov experiment. In principle, this could be used to identify the showers generated by  $\gamma$ -ray primaries if the energy is independently estimated.

In rest of the paper we will be discussing the inter-shower photon density fluctuations only.

### 5.2 Inter-shower fluctuations

Figure 6 shows the variation of the relative shower to shower photon density fluctuations as a function of core distance for 5 different primary energies (a) of 50, 100, 250, 500 & 1000 GeV for  $\gamma$ -ray primaries and (b) 150, 250, 500, 1000 and

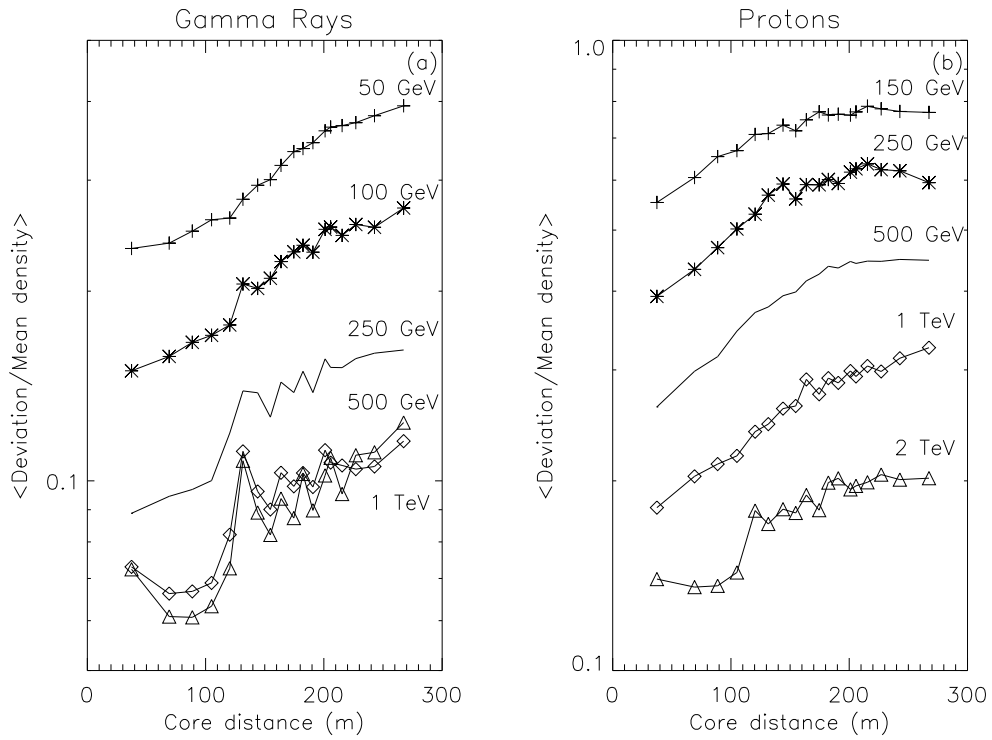


Figure 5: Ratio of the magnitude of deviation to the mean photon density as a function of core distance for (a)  $\gamma$ - rays and (b) protons. Mean densities are calculated for groups of 10 consecutive detectors arranged with increasing core distance. Ratios are averaged over 400 showers for 50 GeV  $\gamma$ - rays and 150 GeV protons, 200 showers for 100 GeV  $\gamma$ - rays, 50 showers for 1 TeV  $\gamma$ - rays and 2 TeV protons. 100 showers are used for the rest.

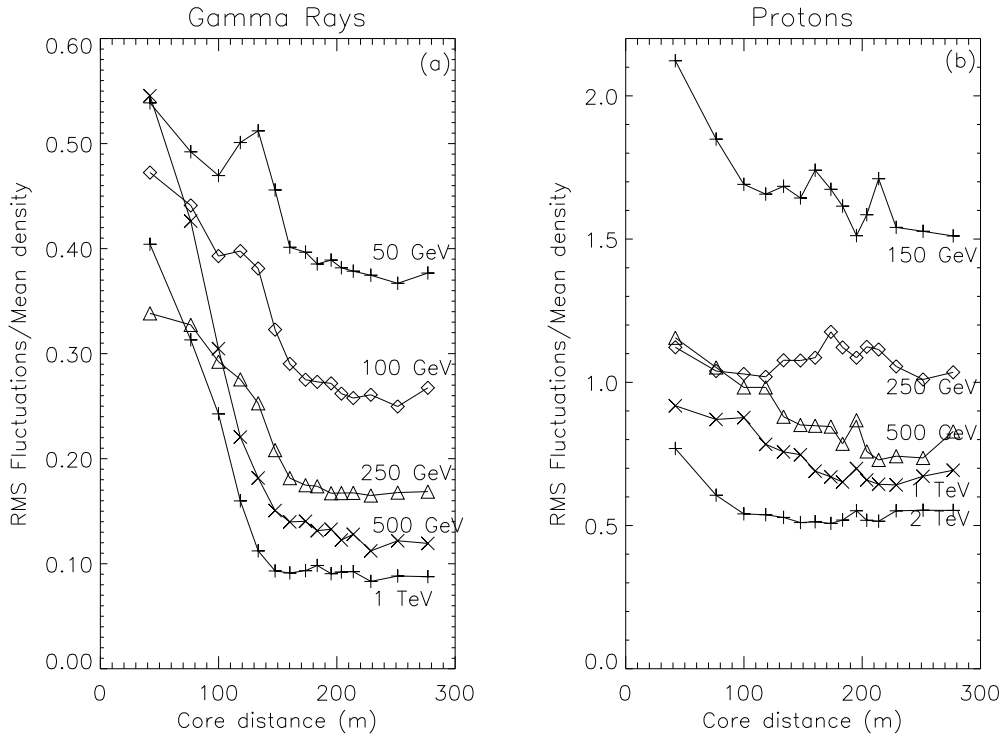


Figure 6: Ratios of non-statistical RMS values to the mean number of Čerenkov photon densities as a function of core distance at five different energies of primary (a)  $\gamma$ - rays and (b) protons. The relative fluctuations for proton primaries are higher and seem to decrease with increase in primary energies in cases of both protons and  $\gamma$ - rays.

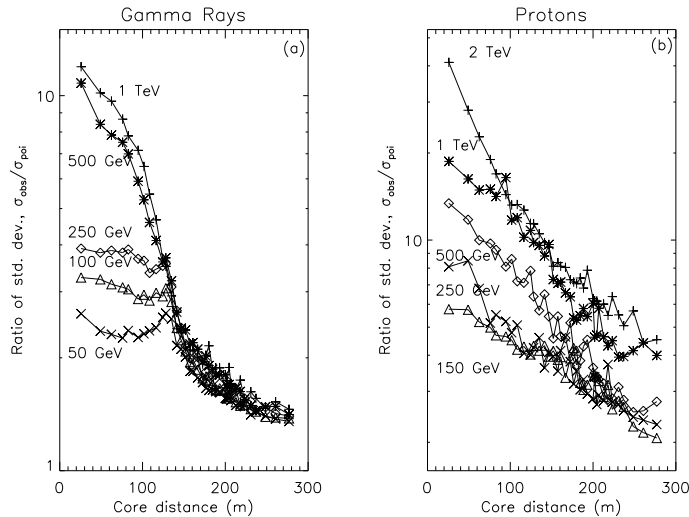


Figure 7: Ratio of the observed RMS fluctuations to Poissonian fluctuations for (a)  $\gamma$ - ray and (b) proton primaries of various energies as a function of core distance.

2000 GeV for protons. The relative fluctuations are measured as a ratio of non-statistical RMS values to the mean number of photons detected at a detector of area  $4.45 \text{ m}^2$ . In general the RMS fluctuations are functions of mean densities. In order to remove this dependence the non-statistical component of the fluctuations is estimated assuming that the total fluctuation is given by the quadratic sum of the statistical (or Poissonian) and non-statistical components. It has been verified that the ratio of the non-statistical component of the RMS fluctuations to the mean value of the density over all the showers ( $r$ ) is independent of detector size and spacing. The relative fluctuations at all primary energies are seen to decrease with increasing core distance and reach a constant value beyond the hump region. The increased fluctuations in the pre-hump region are due to correlated emission from high energy electrons (see section 7.1 for more details).

For a given primary the relative fluctuations decrease with increasing primary energy as observed by others (Ong, 1995). This is primarily due to the reduced electron number fluctuations at higher primary energies. The decrease in the degree of fluctuations with increasing primary energy is monotonic only beyond the hump region. It decreases monotonically up to a primary energy of say 250 GeV for  $\gamma$ - ray primaries at all core distances. It can be seen from fig. 6 that at primary energies of 500 GeV and 1 TeV the fluctuations within the hump region increase dramatically exceeding the values at lower energies. Table 2 shows the average production heights of Čerenkov photons at 3 core distance ranges for 3 different primary energies viz. 100, 500 and 1000 GeV. It can be seen that the differences in the Čerenkov production heights for near core distances and hump region increase with increasing energy. This is due to the production of Čerenkov

Table 2: The average production height (km) of Čerenkov photons at a given core distance range resulting from vertically incident  $\gamma$ - rays of three different energies at the top of the atmosphere. At near core distances the Čerenkov photons are produced at relatively lower heights especially at higher energies through direct emission of Čerenkov photons by the surviving electrons.

Core distance (m)	100 GeV	500 GeV	1000 GeV
30-60	9.0	7.3	6.5
115-130	10.6	9.3	8.6
220-250	9.9	8.5	7.8

photons by the electrons which survive to this height. At higher energies larger number of electrons survive closer to the observation level and produce Čerenkov photons directly before undergoing Coulomb scattering and thus contribute to the increased photon density fluctuations within the hump region. For example, the direct Čerenkov photons reaching the core distance of about 45 m are originated at a height of 2.2 km ( $\sim 800gcm^{-2}$ ). At this height, a total of nearly 16 and 44 electrons (and positrons) of average energy of 0.04 GeV survive in case of 500 GeV and 1000 GeV  $\gamma$ - ray showers, respectively. They form nearly 3% and 4% of the maximum number of electrons produced. Photons emitted by some of these electrons could be correlated and hence contribute significantly to the fluctuations.

Table 3 shows the average arrival angles of Čerenkov photons at different core distance ranges for 3 different  $\gamma$ - ray primary energies. The increasing average arrival angle with increasing primary energy demonstrates that Čerenkov emission from electrons has a larger lateral spread at higher energies. At core distances past the hump the Čerenkov photons are produced mainly from scattered electrons (see section 7.2 for more details) and hence their fluctuations decrease with increasing primary energy.

It can be seen that the magnitude of fluctuations for proton primaries is higher by a factor of 3–5 compared to those for  $\gamma$ - ray primaries. The difference seems to increase with increasing energy. At a  $\gamma$ - ray energy of 50 GeV this ratio is close to 3 while it is around 5 for 1 TeV  $\gamma$ - rays. The large rms fluctuations in the case of proton primaries are mainly due to the increased relative fluctuations in the electron number in the atmosphere. This is much more significant compared to the Poissonian component. Further, the near constant relative fluctuations show that the contribution from correlated emission from high energy electrons is small (see section 7.1 for more details).

Figure 7 shows the ratio of the observed total RMS fluctuations (as against non-statistical fluctuations in fig. 6) to the expected fluctuations if they were purely Poissonian, for  $\gamma$ - rays and protons as a function of core distance. For  $\gamma$ - rays, observed fluctuations are larger than Poissonian at all energies upto

Table 3: The average angle of arrival (deg.) of Čerenkov photons at different core distance ranges, resulting from vertically incident  $\gamma$ - rays of three different energies at the top of the atmosphere. At near core distances the mean arrival angles increase with increasing primary energy because of direct emission of Čerenkov photons by the surviving electrons, which have a larger lateral spread.

Core distance (m)	100 GeV	500 GeV	1000 GeV
30-60	0.38	0.47	0.53
115-130	0.73	0.81	0.87
220-250	1.46	1.73	1.91

the hump, approaching Poissonian value beyond the hump, although they are always higher than Poissonian in the core distance range considered here. In case of protons, relative fluctuations are much larger than those for  $\gamma$ - rays and decrease with increasing core distance. In this case too the tendency to converge to Poissonian fluctuations at large core distance is perhaps present probably at much larger core distances. For  $\gamma$ - ray primaries relative RMS fluctuations seem to be independent of energy of the primary beyond the hump, whereas in case of protons the fluctuations increase with increase in energy. In summary, the density fluctuations are significantly non-Poissonian and more prominent at near core distances.

The relative fluctuations shown in fig. 7 are not independent of the mean density. It can be shown that

$$\sigma_{RMS}^T / \sigma^P = \sqrt{(1 + \sigma_{RMS}^{NS} r)} \quad (1)$$

where  $\sigma_{RMS}^T$  and  $\sigma_{RMS}^{NS}$  are the total and non-statistical RMS fluctuations and  $\sigma^P$  is the Poissonian fluctuations given by the square root of the mean density. Fig. 7 shows only the relative fluctuations for two types of primaries.

It has been suggested in the past (Vishwanath, et al., 1993) that these non-statistical fluctuations could be measured in an observation and used to improve the signal to noise ratio. However, it was routinely assumed that for  $\gamma$ - ray primaries the fluctuations are Poissonian (Rao & Sinha, 1988; Hillas and Patterson, 1987). Such conclusions based on the assumption of Poissonian fluctuations in the photon densities in the lateral distribution have to be revised.

## 6 Other statistical parameters

Figure 8 shows the variation of the higher statistical moments like the skewness (a & b) and kurtosis (c & d) of the frequency distribution of Čerenkov photon densities as a function of core distance for  $\gamma$ - ray (a & c) and proton primaries (b & d). Each of the plots has two curves for two different primary energies as indicated. For  $\gamma$ - ray primaries the density fluctuations show finite positive

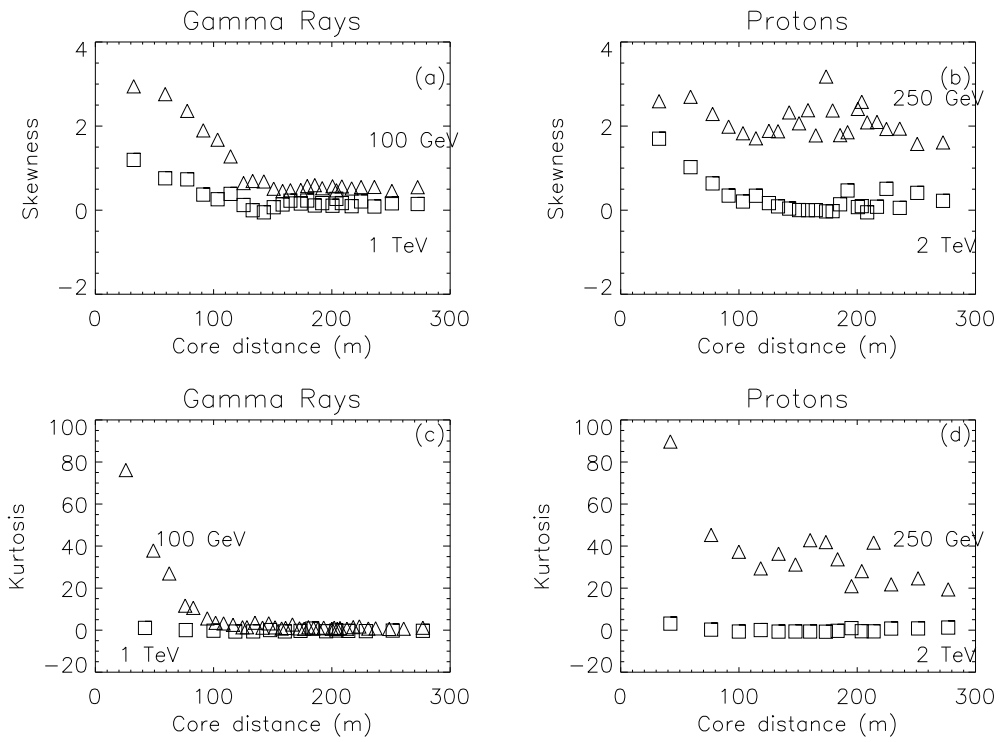


Figure 8: Variations of the third and fourth moments of the Čerenkov photon density fluctuations as a function of core distance at two different energies for (a) & (c)  $\gamma$ - rays and (b) & (d) protons.

skewness before the hump region showing that the distributions have a longer tail towards the higher densities. The observed skewness is more than the statistical value of  $\frac{1}{(\text{mean})^{\frac{1}{2}}}$ . The Čerenkov photons within the hump region are contributed to by two different sources: (i) electrons past the shower maximum emitting Čerenkov photons directly before undergoing scattering, which fill the region between core and the hump and (ii) Čerenkov photons emitted by lower energy electrons after one or more Coulomb scatterings. Larger skewness seen in case of lower energy  $\gamma$ - ray primaries is because of the relative fluctuations in the number of electrons surviving below shower maximum. For lower energy  $\gamma$ - rays the mean number of surviving electrons is much smaller compared to higher energy  $\gamma$ - rays and hence subject to larger fluctuations resulting in larger skewness. At smaller mean values the electron number distribution is asymmetric leading to a large skewness. After the hump the skewness becomes zero as the distribution becomes more symmetric. This could be understood since the photons beyond the hump region are mainly from Coulomb scattering of low energy electrons. In addition, this dependence of the skewness on the core distance gets diluted at higher primary energies. For proton primaries, however, there is no marked core distance dependence as the distribution has rather large positive skewness uniformly at all core distances at lower primary energies, which seem to decrease fast with increasing energy. In addition, isolated high energy electron tracks give rise to excessive photon densities (section 7.1) leading to a large positive skewness.

Similarly the distributions at lower primary energies seem to show a positive non-statistical kurtosis, indicating that the distributions are sharply peaked compared to normal distribution and this effect vanishes at higher energies.

## 7 Possible Origin of fluctuations

There are several possible sources of Čerenkov photon density fluctuations as seen at an observation level which is relatively far from the shower maximum.

### 7.1 Non-independent production processes

A single relativistic electron track can emit several Čerenkov photons which are generically related and hence the conventional statistics does not apply because of lack of independence among these photons. These Čerenkov photons are strongly correlated and consequently give rise to large non-Poissonian fluctuations at the observation level (Sinha, 1995). Occasional local anomaly could be caused by high energy electron track accentuating the above effect. This is demonstrated in fig. 9, which shows the number of detected Čerenkov photons in (a) pre-hump, (b) hump and (c) post-hump regions, at distances of 32 m, 123 m and 234 m from the core, for 100 showers produced by  $\gamma$ - ray primary with energy of 500 GeV. Also shown in the figure is average electron energy at atmospheric depth



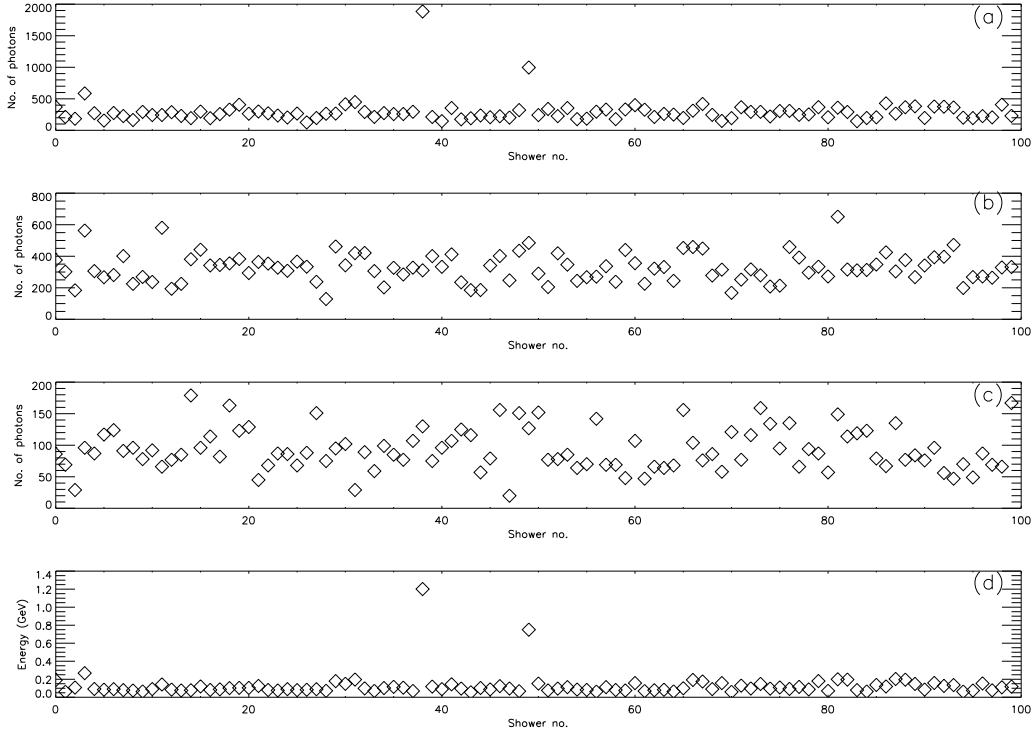


Figure 9: This figure shows the total number of Čerenkov photons detected by a detector in (a) pre-hump, (b) hump and (c) post-hump regions, at a distance of 32, 123 and 234m respectively from the core. Average energy of electrons at an atmospheric depth of  $400 \text{ gm cm}^{-2}$  is shown in (d). The primary  $\gamma$ - ray energy is 500 GeV.

of  $400 \text{ gm cm}^{-2}$ , which is just below shower maximum (at about  $320 \text{ gm cm}^{-2}$ ). Higher average energy of electrons seen in shower no. 38 and 49 is correlated with significantly higher photon densities in pre-hump region. Hump and post-hump regions do not have such significant excess in photon densities. Thus showers with larger average energy for electrons produce distinctly higher density of Čerenkov photons only in pre-hump region. This explains the larger fluctuations seen in fig. 5 for all energies of  $\gamma$ - ray primaries in pre-hump region. Fig. 10 shows the correlation between Čerenkov photon density and average electron energies at an atmospheric depth of  $400 \text{ gm cm}^{-2}$  as a function of core distance. Larger correlation in pre-hump region is evident. By tracing the lateral extent of these large density fluctuations it has been found that the linear length scale varies from about 80 m to 120 m with a mean value of about 100 m. This characteristic length scale does not seem to be a sensitive function of  $\gamma$ - ray energy.

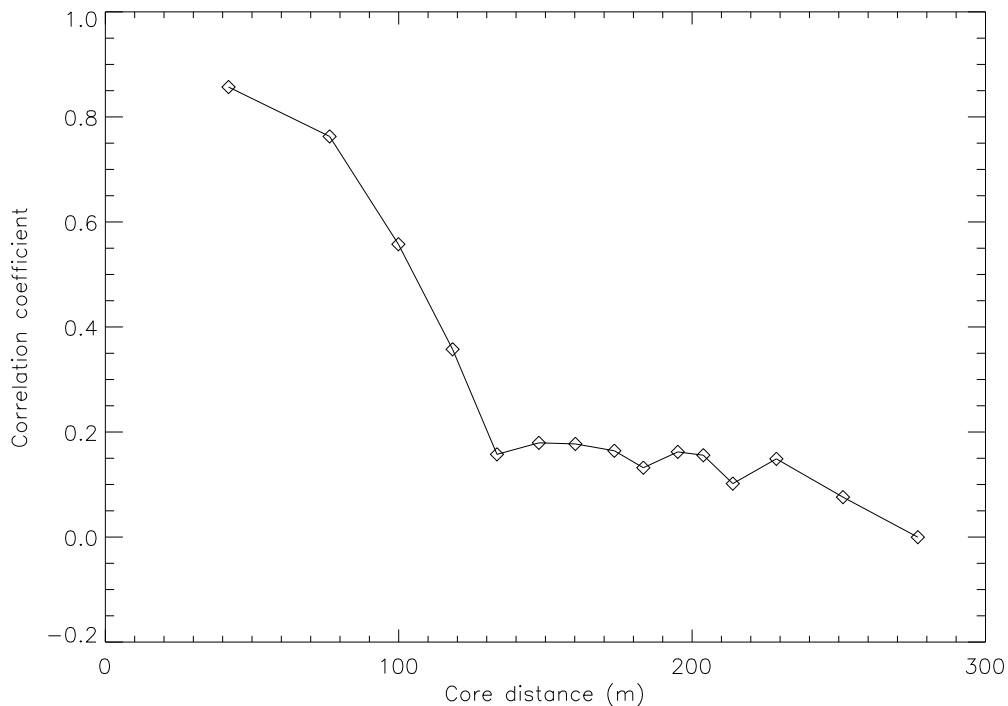


Figure 10: Correlation between number of detected Čerenkov photons per detector and average energy of electrons at atmospheric depth of  $400 \text{ gm cm}^{-2}$  as a function of core distance. 100 showers of 500 GeV  $\gamma$ - rays were used. Points denote averages over 25 consecutive detectors when arranged in increasing order of core distance.

Table 4: The average angle of arrival of Čerenkov photons at a given core distance resulting from vertically incident  $\gamma$ - rays of energy 100 GeV at the top of the atmosphere. This, when compared with the maximum core distance of direct Čerenkov photons, demonstrates the need for Coulomb scattering of low energy electrons to account for the observed photon densities (see text for details).

<b>Core Dist.</b>	<b>Aver. angle</b> ( $^{\circ}$ )	<b>Atm. Height</b> (derived.) (km)	<b>Atm. Height</b> (sim.) (km)	<b>Atms Depth</b> $g \text{ cm}^{-2}$	<b>Čeren. Angle</b> ( $^{\circ}$ )	<b>Max. core dist.</b> (m)
30-60 m	0.38	6.94	8.96	421	0.94	114.0
115-130 m	0.73	9.42	10.6	293	0.81	132.3
220-250 m	1.46	9.3	9.88	299	0.81	131.8

Table 5: The average angle of arrival of Čerenkov photons at a given core distance resulting from vertically incident protons of energy 250 GeV at the top of the atmosphere. This, when compared with the maximum core distance of direct Čerenkov photons, demonstrates the need for Coulomb scattering of low energy electrons to account for the observed photon densities (see text for details).

<b>Core Dist.</b>	<b>Aver. angle</b> (°)	<b>Atm. Height</b> <b>(derived)</b> (km)	<b>Atm. Height</b> <b>(sim.)</b> (km)	<b>Atm. Depth</b> $g\text{ cm}^{-2}$	<b>Čeren. Angle</b> (°)	<b>Max. core dist.</b> (m)
30-60 m	0.60	4.43	6.5	593	1.08	83.7
115-130 m	0.96	7.15	6.96	409	0.93	116
220-250 m	1.46	9.3	7.58	299	0.81	131

## 7.2 Coulomb scattering of electrons

The Coulomb scattering of low energy electrons can lead to density fluctuations as the Čerenkov photons that are emitted by an electron could be diverted to a different location on the ground due to scattering of the parent electron in air. However in general Coulomb scattering tends to smear the fluctuations caused by processes mentioned in section 7.1. Table 4 demonstrates the effect of scattering on the observed lateral distribution of Čerenkov photons in the case of a  $\gamma$ -ray primary of 100 GeV incident vertically at the top of the atmosphere. The second column lists the average observed arrival angle of Čerenkov photons at a core distance range given in column 1. The core distances were suitably chosen to represent pre-hump, hump and post-hump regions respectively. Column 3 lists the atmospheric height where the Čerenkov photons arriving at the angle shown in column 2 could have originated. Column 4 shows the average atmospheric height, estimated from the simulation results, which contributes Čerenkov photons at core distance range shown in column 1. Column 5 shows the atmospheric depth at the height shown in column 3 and column 6 shows the Čerenkov angle at that height. Column 7 is maximum core distance at which Čerenkov photons reach the observation level. Only at the hump region the core distances of the observed photons (column 1) and those of the direct hit Čerenkov photons (column 7) agree well indicating that these photons are emitted by electrons without undergoing significant Coulomb scattering. While the directly emitted Čerenkov photons would not have reached the observed core distances in pre- and post-hump regions if the emitting electrons had not undergone Coulomb scattering significantly. The difference between the derived and observed effective production heights of Čerenkov photons in pre-hump and post-hump regions (columns 3 and 4) again demonstrates the dominance of Coulomb scattering of electrons.

Table 5 gives a similar information for proton primaries of energy 250 GeV. Here also the photons at a core distance of around 120 m have their Čerenkov

Table 6: Correlation coefficients of the shower size with the height of shower maximum and height of first interaction point from a sample of 300 showers each of  $\gamma$ - ray and proton primaries.

Primary species	Corr. Coeff. of shower size with shower maximum ( $g\text{ cm}^{-2}$ )	Corr. Coeff. of shower size with height (km) of first interaction
$\gamma$ - rays (100 GeV)	0.79	-0.7
$\gamma$ - rays (1000 GeV)	0.83	-0.71
Protons (250 GeV)	0.16	-0.11
Protons (2000 GeV)	0.23	-0.26

angles and the arrival angles equal. At shorter core distances the average arrival angles are larger than those for  $\gamma$ - ray primary because of the larger lateral spread of the electrons in the case of proton primaries. However the need for significant Coulomb scattering of electrons is borne out by the difference in the maximum reach of the Čerenkov photons and the observed core distance.

### 7.3 Fluctuations in the height of first interaction

The height of first interaction of a primary proton or a  $\gamma$ - ray in the atmosphere that initiates the cascade fluctuates within one interaction length. The extent of fluctuation is decided by the radiation length in air ( $37.15gcm^{-2}$ ) in the case of  $\gamma$ - ray primaries and the interaction mean free path ( $70gcm^{-2}$ ) in the case of protons. Fluctuations in the point of first interaction in turn lead to the fluctuations in the height of the shower maximum. A shower with a maximum at a point lower down in the atmosphere effectively comes closer to the observation level and hence results in higher number of Čerenkov photons since the Čerenkov yield is an increasing function of refractive index. Thus fluctuations in the height of the shower maximum give rise to density fluctuations at the observation level. Both the height of first interaction as well as the height of shower maximum for a primary  $\gamma$ - ray of given energy is correlated with shower size (see table 6). However, such a correlation is absent in the case of proton primaries. Table 7 lists the magnitude of fluctuation of these parameters for a 100 GeV  $\gamma$ - ray incident vertically at the top of the atmosphere.

The Čerenkov photon density fluctuations at the observation level is a result of multiple components. While it is not possible to quantify the contributions from all the processes separately, one can estimate the contribution from the fluctuations in the height of shower maximum. A sample of 500  $\gamma$ -ray showers of energy 100 GeV have been simulated and a distribution (bin width = 1 km equivalent to  $\sim 4\text{ gm cm}^{-2}$  at an altitude of  $\sim 25\text{ kms}$ ) of these showers is generated based on their height of first interaction in the atmosphere. The mean

Table 7: Magnitude of fluctuations in the height of first point of interaction, shower maximum and the number of Čerenkov photons detected at observation level for a 100 GeV  $\gamma$ - ray incident vertically at the top of the atmosphere.

<b>Parameter</b>	<b>Mean value</b>	<b>RMS fluctuations</b>	<b>Relative RMS fluctuations</b>
Height of first interaction (m)	25582.2	7962.3	31.1%
Height of shower maximum ( $g\text{ cm}^{-2}$ )	260.6	65.70	25.3%
No. of Čerenkov photons detected at the observation level	11480	3050	26.6%

RMS value of the fluctuations of the shower size in the bins around the peak of its distribution is computed to be 3%, compared to 5.2% for the totality of the showers. This value is presumably free from the contribution to fluctuations from the fluctuations in the height of first interaction. This value does not vary significantly if we reduce the bin width by a factor of 2. Hence the fluctuations in the height of first interaction contributes significantly to the observed fluctuations in the shower size for  $\gamma$ - ray primaries.

A similar estimate for proton primaries shows that the contribution from the fluctuations in the height of first interaction is negligible showing that the contributions from other processes dominate. In the case of proton primaries, it was possible to freeze the height of first interaction at the mean value for 250 GeV proton primaries. The value of the RMS fluctuations in the shower size after fixing the height of first interaction is 29.2%, compared to 30% obtained without doing so, confirming the above conclusion.

## 7.4 Electron number fluctuations

In an attempt to further understand the relative contributions to the observed density fluctuations at the observation level, we studied the fluctuations in the production height of Čerenkov photons for  $\gamma$ - ray and proton primaries. Fig. 11(a) shows the production height distribution of Čerenkov photons generated by 100 GeV  $\gamma$ - rays, averaged over 50 showers. Error bars correspond to RMS deviations and are clearly non-statistical. Electron growth curve is also shown in the fig 11(c). The photon and electron growth curves are very similar as expected. Both the number of Čerenkov photons and electrons peak at a height of around 10 km, which is the shower maximum. Fluctuations in the number of Čerenkov photons at a given height in the atmosphere can be attributed to those in the number of electrons, which in turn owe their origin to the production kinematics. It may be noticed from plots in 11(b) & (d) where relative rms deviations are plotted as a function of height, that the fluctuations are relatively larger after the shower maximum.

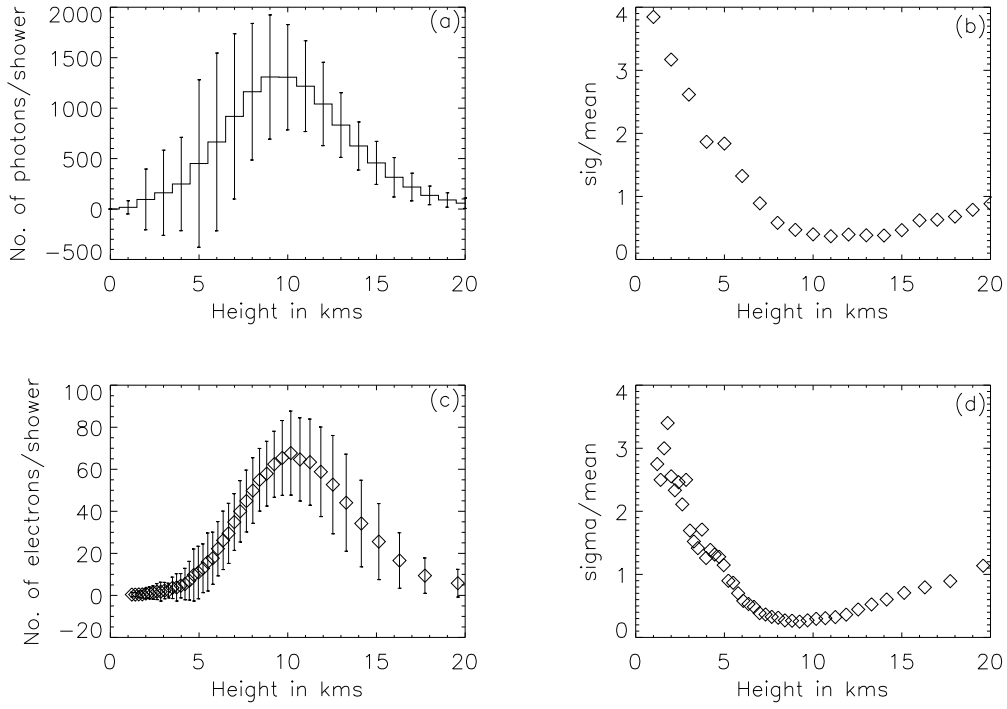


Figure 11: Production height distribution of (a) Čerenkov photons and (c) electrons generated by 100 GeV  $\gamma$ -ray primaries. The error bars indicate the rms deviations. The plots on the right show the relative errors measured as a ratio of the average number (over 50 showers) for (b) photons and (d) electrons. The number on the y-axis of (a) and (c) could be multiplied by 2 to include positrons as well.

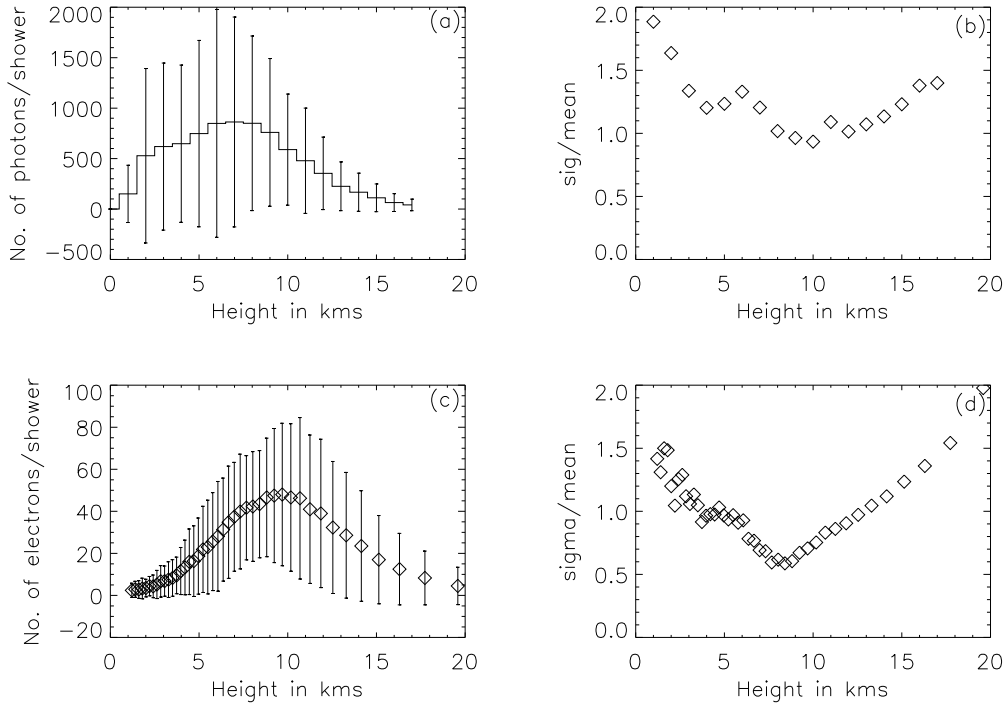


Figure 12: Production height distribution of (a) Čerenkov photons and (c) electrons generated by 250 GeV proton primaries. The error bars indicate the rms deviations. The plots on the right show the relative errors measured as a ratio of the average number (over 50 showers) for (b) photons and (d) electrons. The number on the y-axis of (a) and (c) could be multiplied by 2 to include positrons as well.

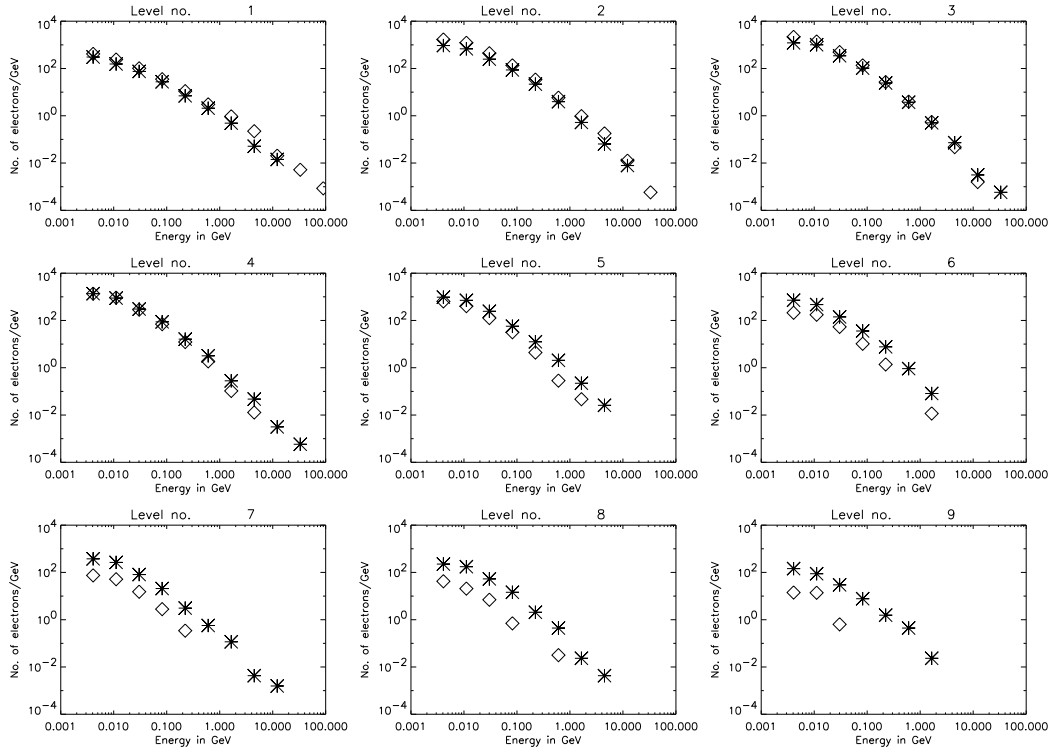


Figure 13: Averaged electron energy spectra (diff) at 9 different atmospheric depths  $100\text{-}900\text{ g cm}^{-2}$  during the shower development for  $\gamma$ - ray(diamonds) and proton(stars) primaries of energy 100 & 250 GeV respectively.

Similar distributions averaged over 50 showers of protons of energy 250 GeV are shown in fig. 12. Here, it may be noticed that the magnitude of fluctuations is much larger compared to those of  $\gamma$ - rays. This is because in the case of proton primaries, the source of electrons is pair production by  $\gamma$ - rays which are the decay products of  $\pi^0$  mesons produced in hadronic interactions. While charged pions could decay to muons which in turn decay to electrons. The fluctuations in the multiplicities of the pion secondaries and their energy spectra combined with the fluctuations due to larger hadronic interaction mean free path (which is nearly twice the radiation length in air) of protons lead to larger electron number fluctuations in the case of proton primaries. The shower development also sustains over a longer distance in the atmosphere for the same reason. The FWHM of the shower development curve for  $\gamma$ - ray and proton primaries are 8 and 10 km respectively. This is due to the finite transverse momentum of  $\pi^0$  secondaries which is about  $0.3\text{ GeV}/c$  in the case of proton primaries.



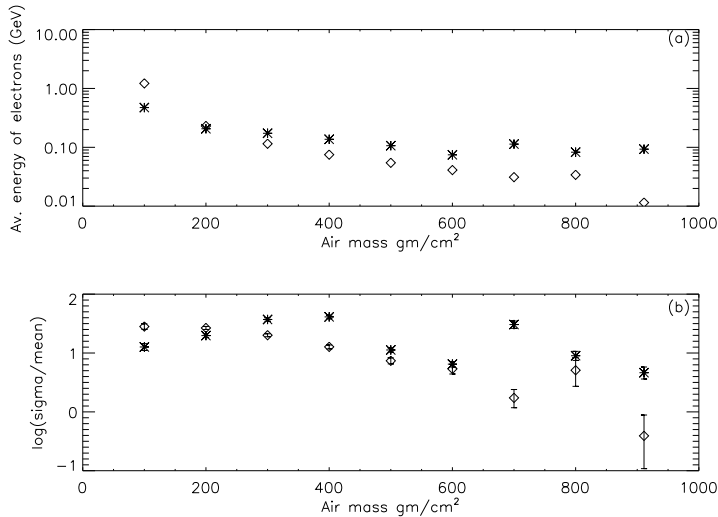


Figure 14: (a) Average electron energy at 9 different atmospheric depths 100-900  $g\text{ cm}^{-2}$  during the shower development for  $\gamma$ -ray (diamond) and proton (star) primaries of energy 100 & 250 GeV respectively. (b) Ratio of RMS deviation to average energy for  $\gamma$ -ray and proton primaries.

## 7.5 Electron energy spectra at various atmospheric depths

Another important contribution to fluctuations comes from the fluctuations in the electron energy and their spectra during the shower development. Figure 13 shows the average energy spectra of electrons (averaged over 50 showers) at 9 different depths (100 - 900  $g\text{ cm}^{-2}$ ) in the atmosphere, both for proton (250 GeV, stars) and  $\gamma$ -ray primaries (100 GeV, diamonds), incident vertically at the top of the atmosphere. Figure 14(a) shows the variation of the average energy of the electrons (calculated as the arithmetic mean of all the electron energies), as a function of atmospheric depth. While the energy spectra seem to be very similar in shape for  $\gamma$ -ray and proton primaries, the average energy after the shower maximum is relatively higher for proton primaries since their height of shower maximum is past that for  $\gamma$ -ray primaries. For the same reason the number of surviving electrons also is relatively larger in the case of proton primaries. The relative fluctuations in the average energy shown in fig. 14(b) indicate the RMS fluctuations which propagate down to those in the number of Čerenkov photons at the observing level. It may be noted that the relative RMS fluctuations in the average electron energies at various atmospheric depths are very similar in the case of  $\gamma$ -ray and proton primaries. Hence the increased fluctuations in the Čerenkov photon densities for proton primaries is mainly the result of increased fluctuations in the electron number during the shower development.

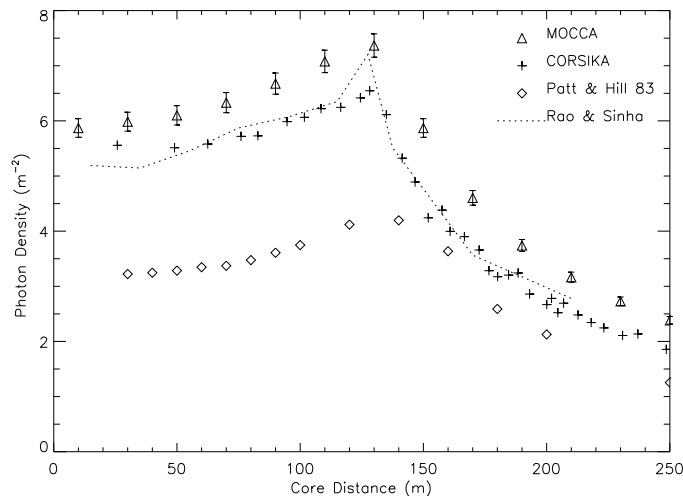


Figure 15: Average lateral distributions of Čerenkov photon densities resulting from vertically incident  $\gamma$ - rays of energy 100 GeV. The average of 200 showers are shown as computed by CORSIKA, MOCCA, Rao & Sinha simulation package and Patterson & Hillas calculations.

## 8 Comparison with other simulations

### 8.1 Average lateral distributions

Here we compare the average (over 200 showers) lateral distributions of Čerenkov photons for  $\gamma$ - ray primaries of energy 100 GeV obtained using CORSIKA, with (a) that obtained by Ong et al. (1995) using a package called MOCCA (Hillas, 1985) (b) a package developed by Rao & Sinha (1988) and (c) the earlier calculations by Patterson & Hillas (1983). The average lateral distributions of Patterson & Hillas were originally made for sea level. The expected density for Pachmarhi altitude (using the estimates of Rao & Sinha (1988)), is around 30% higher than that for sea-level. However, the core distance of the hump also reduces at higher altitudes and there is no easy way to correct for this effect. Results are shown in the fig. 15. We have corrected the lateral distribution obtained with CORSIKA for atmospheric attenuation of Čerenkov photons using the same attenuation factor as used by Rao & Sinha (Acharya, 1997). All the three lateral distributions (a), (b) and (c) agree within errors while (d) agrees with the rest only beyond the hump region. It may be mentioned that the estimates by Rao & Sinha do not take into account the effects of geomagnetic field. Slightly higher photon density obtained by Ong et al. may be due to the differences in Čerenkov bandwidth and altitude used by them. The calculations of Patterson & Hillas (1983) are underestimated by about 22% compared to CORSIKA, even after accounting for the differences in the observation levels. The photon densities

as well as the hump agree reasonably well in cases a, b and c, showing that all the three simulation packages include correct treatment of Coulomb scattering of high energy electrons and their relative track length integrals.

## 8.2 Average shower size

As seen in section 4 the shower size (measured in terms of the total number of Čerenkov photons produced) for 100 GeV  $\gamma$ - ray primaries obtained using CORSIKA is about  $4.3 \times 10^6$  photons and the ratio of RMS deviation to the average number of Čerenkov photons is 5%. For the same  $\gamma$ - ray energy Ong et al. (1995) have estimated the total number of Čerenkov photons within 150 m from the shower axis to be around  $4.78 \times 10^5$  and the ratio of RMS deviation to the number of Čerenkov photons to be 34%. The difference between the numbers are mainly due to the difference in collection area, which is a circle of radius 150 m centered at the core in case of Ong et al., whereas the numbers given by us correspond to the entire pool. Using detected number of Čerenkov photons at various core distances and using a quadratic fit to the lateral distribution, we estimate the number of Čerenkov photons within 150 m from shower axis to be around  $6.27 \times 10^5$ . Considering the atmospheric attenuation it reduces to  $3.49 \times 10^5$  photons, which is consistent with the number given by Ong et al. Also using the number of detected Čerenkov photons we have estimated the ratio of RMS deviation to the number of Čerenkov photons within 150 m of shower axis to be about 28%. Considering an unequal radial distribution of the detector array used in our calculations, this number is also consistent with that obtained by Ong et al.

## 8.3 Effect of geomagnetic field

It has been found that the effect of wavelength dependent absorption of Čerenkov photons in the atmosphere is independent of core distance and hence it does not affect the prominence of the hump. The difference between the average lateral distributions derived from CORSIKA taking into account the local geomagnetic field and without taking into account, is shown in figure 16(a). It shows that the deflection of electrons in the Earth's magnetic field would dilute the prominence of the hump by broadening it as expected (Porter, 1973). The electron deflection in the magnetic field is equivalent to increased Coulomb scattering and hence is expected to produce more fluctuations in the observed photon densities. Figure 16(b) shows the relative rms fluctuations with and without taking into account the presence of the geomagnetic field confirming the above conclusion. Also shown in the plot are relative RMS fluctuations if they were purely Poissonian in origin.

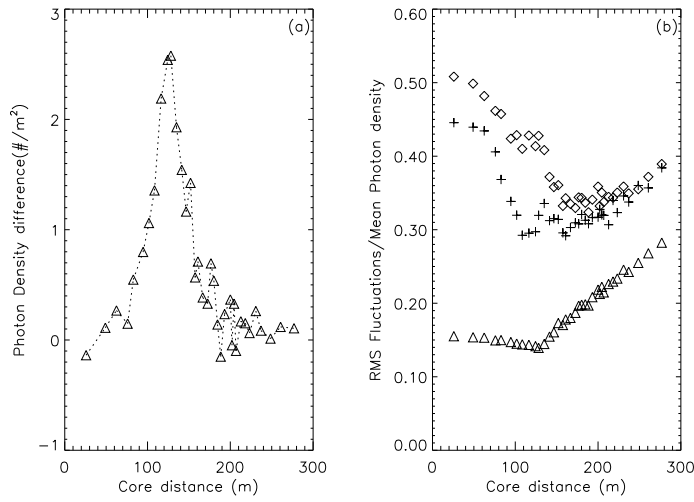


Figure 16: (a) The effect of the geomagnetic field on the average lateral distribution of Čerenkov photons. The difference between the Čerenkov photon densities without and with geomagnetic field is plotted as a function of core distance. The increased prominence of the hump in the absence of the field is clearly seen. The primary  $\gamma$ -ray energy is 100 GeV. See text for details. (b) The change in the relative fluctuations of Čerenkov photon densities as a function of core distance due to the presence of geomagnetic field. Relative fluctuations with geomagnetic field are indicated by diamonds, without field by + and Poissonian fluctuations by triangle.

## 8.4 Density fluctuations

There are very few results available in the literature on the study of fluctuations of Čerenkov photons. It has been known qualitatively that the shower to shower variations are relatively higher in the case of showers initiated by hadrons compared to those generated by  $\gamma$ - rays. This is mainly because the electromagnetic cascades, which contribute to Čerenkov photon density in the case of hadronic primaries, are the result of a superposition of several  $\gamma$ - ray cascades initiated by the decay products of  $\pi^0$  mesons whose numbers are subjected to fluctuations. However, no serious attempt was made to compare these fluctuations quantitatively and qualitatively in the past.

Sinha (1995) studied these fluctuations only for  $\gamma$ - ray primaries of energies 100, 500 and 2000 GeV. There is a qualitative agreement between these calculations and the present work in the sense that the degree of fluctuations decrease from the core going through a minimum at around the hump region and then showing a slight increase at large core distances. As the photons at around the hump are contributed mainly by higher energy electrons ( $E_e > 1 \text{ GeV}$ ) they will undergo relatively less scattering and hence are subjected to minimum fluctuations. At small core distances the asymmetric distributions of densities lead to larger fluctuations, while at large core distances the residual fluctuations seen are due to Coulomb scattering. Since the estimates by Sinha are for sea level the degree of fluctuations cannot be compared quantitatively. Our estimates of relative fluctuations as a function of core distance shows no agreement with the Poissonian fluctuations at any core distance while Sinha (1995) observes that beyond the hump region the observed fluctuations are consistent with Poissonian. Since the Coulomb scattering of low energy electrons is responsible for Čerenkov photons reaching beyond hump region one would expect to see the residual contribution to fluctuations from Coulomb scattering as shown in the present work.

## 9 Conclusions

A systematic study of the fluctuations in the Čerenkov photons generated by  $\gamma$ - ray and proton primaries in the earth's atmosphere and detected at the observation level has been carried out. Such a quantitative estimate of the degree of fluctuations for the two types of primaries and the dependence on the core distance as well as primary energy has been done for the first time here. This type of study is important in planning observations of VHE  $\gamma$ - ray sources based on the measurement of lateral distributions of Čerenkov photons, since these experiments are based on improving signal to noise ratio by rejecting the abundant charged particle background. The large non-statistical fluctuations reported here might reduce the efficiency of rejection.

We have studied the density fluctuations as a function of core distance for

various energies of  $\gamma$ - ray and proton primaries in 50–1000 GeV range. Fluctuations are highly non-statistical and decrease with increasing primary energy in both the cases. Proton primaries show larger fluctuations compared to  $\gamma$ - ray primaries of corresponding energy. In case of  $\gamma$ - ray primaries fluctuations are minimum at the hump region and approach Poissonian beyond the hump region. Proton showers in general show larger fluctuations than  $\gamma$ - ray primaries even in the case of shower size measured in terms of the total number of Čerenkov photons generated.

We have investigated various known sources of fluctuations and tried to evaluate their relative contributions. Effect of geomagnetic field is to deflect electrons and thereby increase the fluctuations. Average electron energies and their spectra at different atmospheric levels during the shower development are found to be similar in case of proton and  $\gamma$ - ray primaries of equivalent Čerenkov yields. Whereas number of electrons at various depths of shower development is found to vary much more for protons compared to  $\gamma$ - rays. We have also studied the effect of variation in the first point of interaction on the shower size fluctuations. It is found to be significant only in the case of  $\gamma$ - ray primaries. Contribution to the fluctuations also comes from Coulomb scattering of low energy electrons past the shower maximum and the intrinsic correlation between the photons emitted by a single electron.

## 10 Acknowledgments

We would like thank Profs. K. Sivaprasad, B. S. Acharya, M. V. S. Rao and P. R. Vishwanath for extensive and illuminating discussions during present work. We would like to thank the anonymous referee whose interesting comments and suggestions helped us improve the quality of this paper.

## 11 References

- Acharya, B. S., Private Communication, (1997)
- Bhat, P. N., *et al.*, Proc. 25th ICRC, Durban, **5**, 105, (1997)
- Browning, R. and Turver, K. E., Nuovo Cimento, 38A, 223 (1977)
- Chadwick, P. M. *et al.*, Proc. 25th ICRC, Durban, **3**, 189, (1997)
- Fegan D., High Energy Astrophysics - Models and Observations from MeV to EeV, Ed. J. M. Mathews, p107, World Scientific, (1994)
- Hillas, A. M., Proc. 19th ICRC, La Jolla, **3**, 445, (1987)

- Hillas, A. M. and Patterson, J. R., Very High Energy  $\gamma$ - Ray Astronomy, Ed. K. E. Turver (Dordrecht: Reidel), 234, (1987)
- Knapp, J. and Heck, D., *EAS Simulation with CORSIKA, V4.502: A User's Manual*, (1995)
- Krys, E. and Wasilewski, A., *Towards a Major Atmospheric Cerenkov Detector-II*, Ed: R. C. Lamb, Calgary, 199, (1993)
- Nelson, W. R., *The EGS4 Code System*, SLAC Report 265 (1985)
- Ong, R. A. et al., *Towards a Major Atmospheric Cerenkov Detector-IV*, ed. M. Cresti, pp. 261, (1995)
- Patterson, J. R. and Hillas, A. M., J. Phys. G: Nucl. Phys., 9, 1433, (1983)
- Porter, N. A., Lett. Nuovo Cimento, 8, 481, (1973)
- Punch, M., *et al.*, Nature, 358, 477 (1992)
- Quinn, J. et al., Proc. 25th ICRC, Durban, **3**, 249, (1997)
- Rao, M. V. S. and Sinha, S., Phys. G: Nucl. Phys.,14, 811, (1988)
- Sinha, S., J. Phys. G: Nucl. Phys., 21, 473, (1995)
- Vacanti , G., et al., Ap J, 377, 467, (1991)
- Vishwanath, P. R. et al., *Towards a Major Atmospheric Cerenkov Detector-II*, Ed: R. C. Lamb, Calgary, 115, (1993)
- Weekes T. C. Physics Reports, **160**, 1, (1988)
- Zatsepin, V. I. and Chudakov, A. E., Sov. Phys.-JETP, 15, 1126, (1962)